Design and Experimental Results for a High-Altitude, Long-Endurance Airfoil

Mark D. Maughmer*
Pennsylvania State University, University Park, Pennsylvania
and
Dan M. Somers†
NASA Langley Research Center, Hampton, Virginia

Currently, there is interest in the development of high-altitude, long-endurance vehicles for a number of missions including communications relaying, weather monitoring, and provision of targeting information for cruise missiles. The preliminary design of such aircraft is complicated, however, by the lack of suitable airfoils. This is due to the fact that such vehicles, unlike those for which the majority of airfoils have been developed in the past, operate at fairly high lift coefficients and at relatively low Reynolds numbers. Thus, to provide realistic airfoil performance information for preliminary design efforts, an airfoil has been designed for an aircraft with missions similar to those noted. The airfoil is unflapped and has a thickness of 15% chord. The design Reynolds number range is 7×10^5 to 2×10^6. Low drag is predicted for lift coefficients ranging from 0.4, which corresponds to a high-speed dash, to 1.5, the maximum endurance condition. Further, the airfoil is designed specifically such that the maximum lift coefficient is unaffected by surface contamination. Consequently, takeoff and landing in rain or with insect residue on the wings should present no special difficulties. The airfoil has been tested in the NASA Langley Low-Turbulence Pressure Tunnel and, with the exception of the maximum lift coefficient prediction, the results generally confirm the theoretical predictions.

Nomenclature

C_D = drag coefficient
C_L = lift coefficient
c = airfoil chord
c_d = section profile-drag coefficient
c_ℓ = section lift coefficient
c_m = section pitching moment coefficient about quarter-chord point
$c_{m,0}$ = section quarter-chord pitching moment coefficient at zero lift
R = Reynolds number based on freestream conditions and airfoil chord
U_∞ = freestream velocity
v = local velocity on airfoil
x = airfoil abscissa
α = angle of attack relative to chord line, deg

Subscripts
ls = lower surface
max = maximum
tr = transition
us = upper surface

Presented as Paper 87-2554 at the AIAA 5th Applied Aerodynamics Conference, Monterey, CA, Aug. 17-19, 1987; received Dec. 28, 1987; revision received July 18, 1988.

*Assistant Professor, Department of Aerospace Engineering. Senior Member AIAA.
†Research Engineer, Fluid Dynamics Branch, Transonic Aerodynamics Division.

Introduction

At the present time, there is a great deal of interest in developing a new class of flight vehicles, both manned and unmanned, for a variety of missions that require operation at high altitudes for extended periods of time. The intended uses for these aircraft include communications relaying, weather monitoring, and provision of targeting information for cruise missiles. Unfortunately, the preliminary design of such vehicles is greatly complicated by the lack of suitable airfoils and airfoil performance data. This is because such vehicles, unlike those for which the majority of airfoils have been developed in the past, operate at fairly high lift coefficients and at relatively low Reynolds numbers.[1] While the problem of airfoils operating at Reynolds numbers below a half-million has been addressed by other recent design efforts,[2,3] there remains a lack of data regarding airfoils operating at slightly higher Reynolds numbers. Thus, in order to provide airfoil data that will allow realistic preliminary design for aircraft operating at these Reynolds numbers, an airfoil has been designed to meet requirements typical of a high-altitude, long-endurance flight vehicle. Although the performance of airfoils at these Reynolds numbers is still dependent on the behavior of laminar separation bubbles, this does not completely dominate the design process, as is the case at the lower Reynolds numbers.

Although the airfoil for a new aircraft that most closely matched the design requirements was once selected from an airfoil "catalog," the state of airfoil design is now at such a level that each new vehicle should have an airfoil tailored specifically to its intended mission. In this way, the highest level of performance possible is attained. The role of the airfoil designer in this case is, as it has always been, to achieve the lift required for the least possible drag. This is not to suggest, however, that the optimum airfoil design is accomplished by minimizing the section drag coefficient or by maximizing the section lift-to-drag ratio. Instead, by making use of modern airfoil design techniques, the designer arrives at

the most suitable airfoil for a particular aircraft by trading off various design requirements. For example, to design an airfoil that minimizes the three-dimensional wing profile drag, obtaining a low section drag coefficient through the achievement of laminar flow must be balanced against the conflicting goal of reducing the wetted-area drag through the attainment of a high maximum lift coefficient, which reduces the required wing area. Clearly, in addition to the wing area, the airfoil characteristics strongly impact other aspects of the configuration. Consequently, to achieve the best possible performance, the airfoil design should be integrated with the aircraft design as shown in the flow diagram presented in Fig. 1.

In considering the aircraft/airfoil design integration depicted in Fig. 1, the most important aspect of matching the airfoil to the aircraft is the airfoil/aircraft design iteration loop. Obviously, the more closely the baseline airfoil data match the mission requirements, the fewer the number of iterations required. Also, it is possible that the airfoil performance needed to satisfy the mission requirements is not achievable. In such cases, the mission specifications must be adjusted and the process repeated.

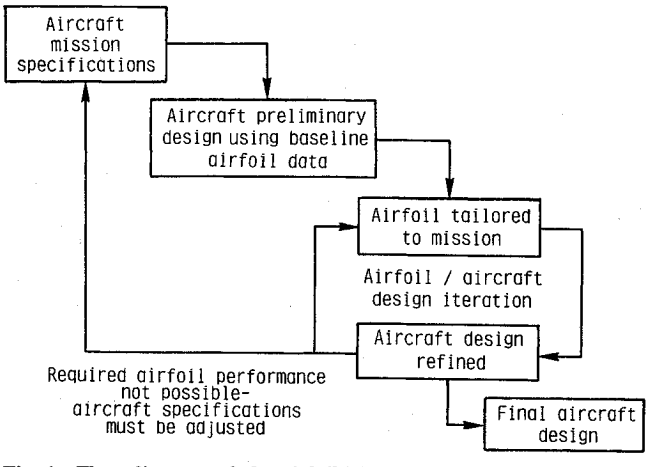

Fig. 1 Flow diagram of the airfoil/aircraft design integration process.

Design Requirements

The first step in designing an airfoil for the high-altitude, long-endurance mission is to define specifications for a representative aircraft. After considering a number of missions and the vehicles proposed to accomplish them, the airfoil design effort was directed toward an aircraft having the following specifications:

Wingspan = 25 m (82 ft)
Gross weight = 19,600 N (4400 lbf)
Empty weight = 9800 N (2200 lbf)
Payload = 1500–4900 N (340–1100 lbf)
Operational altitude = 20,000 m (66,000 ft)
Endurance ≈ 90 h
Range ≈ 32,000 km (20,000 miles)

From performance studies of an aircraft based on the above specifications, it is possible to develop design requirements for the airfoil at any spanwise location. For the aircraft described, the Reynolds number range over which the wing operates is from 0.3×10^6 for the tip at maximum altitude with fuel almost spent to 5×10^6 for the root at sea level with full fuel. Although such a large Reynolds number variation clearly dictates the design of different airfoils along the span, the present effort was limited to the airfoil located at the mean aerodynamic chord. The characteristics of this airfoil, however, should be indicative of those at any other span station. The design requirements for this airfoil are summarized in the form of the section drag polar given in Fig. 2. The upper limit of the low-drag range corresponds to the maximum endurance flight condition ($c_\ell = 1.5$, $R = 0.7 \times 10^6$). The lower limit of the low-drag range corresponds to high-speed dash ($c_\ell = 0.4$, $R = 2.0 \times 10^6$). The design goal is to achieve the lift coefficients required at the key operational points noted with the lowest possible profile drag coefficients. Thus, the desired polar is of the form shown, but moved to the left as far as possible for the given low-drag range. Because of the inability of a low Reynolds number flow to negotiate the large pressure recoveries required for high lift coefficients, the primary challenge presented by these requirements is represented by the maximum endurance flight condition. Finally, it is desirable to achieve a reasonably high maximum lift coefficient for takeoff and landing performance.

In order that the most suitable airfoil for a given aircraft results, it is necessary to guide the design process by quantitatively comparing the performance of different candidate airfoils. On first consideration, because the best aircraft endurance results when $C_L^{3/2}/C_D$ is a maximum, it is often suggested that the airfoil having the highest section value of

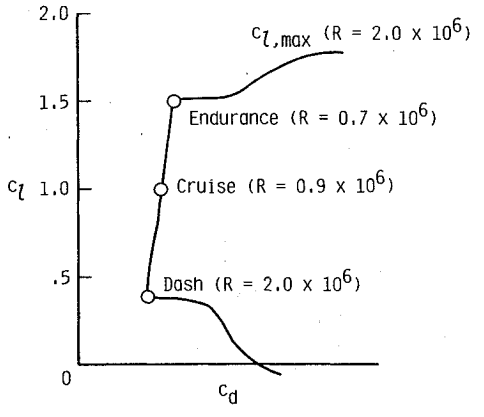

Fig. 2 Design goals for the high-altitude, long-endurance airfoil.

the so-called endurance parameter, $c_\ell^{3/2}/c_d$, offers the best aircraft endurance. In actuality, because of the impact of the airfoil on such things as wing area, tail size, etc., the use of the airfoil having the highest endurance parameter does not necessarily ensure the longest endurance for the aircraft. In fact, because takeoff length is a design consideration for this aircraft, it is found, as developed in detail in Ref. 4, that in order to obtain the maximum aircraft endurance, the airfoil should be designed to maximize the quantity

$$\frac{c_{\ell,\max}}{c_d \text{ at } c_{\ell,\text{operational}}}$$

where $c_{\ell,\text{operational}}$ is the lift coefficient at the operating point considered to be the most critical or significant. For the design under consideration, $c_{\ell,\text{operational}} = 1.5$, which corresponds to the maximum endurance condition. This figure of merit provides a quantitative means of trading off the gain due to decreasing wetted-area wing drag by increasing the maximum lift coefficient against that due to decreasing the section drag coefficient by achieving more extensive laminar flow. It is notable that, if the operational lift coefficient is taken as that corresponding to the minimum section drag coefficient, then this figure of merit is equivalent to the one presented in Ref. 5, which guides the design of the airfoil resulting in the lowest three-dimensional wing profile drag.

To demonstrate the usefulness of the maximum endurance figure of merit, the two drag polars depicted in Fig. 3 should be considered. Whereas the airfoil having performance represented by the solid line has a lower profile drag coeffi-

cient over most of the flight range of interest, the higher maximum lift coefficient of the airfoil represented by the dashed line allows the wing area to be decreased, thereby reducing the wetted-area drag. It should be realized that, while the two polars are very different, it is entirely possible that the two airfoils have the same maximum section endurance parameter or lift-to-drag ratio. Thus, while it is clear that one of these airfoils must offer better aircraft endurance, it is not at all clear which one it is. The figure of merit provides a quantitative means of making the proper choice.

In addition to the previously discussed design considerations, it was also decided that the airfoil should not have a flap, should not produce a large nose-down pitching moment, and should achieve a maximum lift coefficient independent of surface contamination. The reason for restricting the design to an unflapped airfoil is that performance calculations show a substantial penalty for carrying the additional weight of a flap system for long periods of time. Further, based on calculations using maximum lift coefficients attainable without flaps, it was found that runway length requirements for the aircraft were not unreasonable. A moderate pitching moment coefficient was dictated by structural and trim drag considerations. Accordingly, $c_{m,0}$ was constrained to values no more negative than -0.20. The requirement that $c_{\ell,\max}$ be independent of surface contamination was imposed because a decrease in $c_{\ell,\max}$ due to leading-edge roughness can result in undesirable, or even dangerous, behavior. Although this constraint has a strong impact on the achievable $c_{\ell,\max}$, it ensures that the takeoff and landing performance are unaffected by rain, bugs, dirt, etc.

Finally, it should be noted that, although compressibility effects become important when the aircraft is operating at dash speeds at high altitudes, the maximum endurance performance, which is of greatest importance, occurs at Mach numbers below 0.4. Thus, the design process did not consider the effects of compressibility.

Design Procedure

Once the design goals for an airfoil have been thoroughly established, some thought must be given to how those goals are to be realized. As previously noted, the most difficult design challenge in the present case is the attainment of relatively high lift coefficients in conjunction with low Reynolds numbers. In order to achieve these high lift coefficients, the velocities on the upper surface must reach relatively high values. However, the low Reynolds numbers severely limit the amount of pressure recovery that can be achieved without separation. For this design, obtaining high lift coefficients while controlling the amount of upper-surface separation is achieved through the use of a "separation ramp," originally proposed by Wortmann. (See Fig. 4.) While some separation is present for lift coefficients within the operating range, the ramp limits the amount of separation to a small region near the trailing edge. It is not until the lift coefficient approaches its maximum that the separation point moves forward of the ramp and into the main pressure recovery region.

In order to achieve $c_{\ell,\max}$ independent of surface contamination, the airfoil embodies upper-surface distributions which behave as shown in Fig. 5. The velocity distribution for $c_\ell = 1.5$, the upper limit of the low-drag range, is prescribed such that the forward movement of transition from a location just upstream of the main pressure recovery is imminent. Thus, for lower lift coefficients, the pressure gradients are such that transition is confined to the instability region just upstream of the main pressure recovery. For higher lift coefficients, however, the adverse pressure gradients over the forward portion of the airfoil cause the transition to move rapidly toward the leading edge. Consequently, because the maximum lift coefficient is achieved with essentially no laminar flow, it is not influenced by premature transition. The pressure peaks near the leading edge do, however, limit the maximum lift that can be achieved.

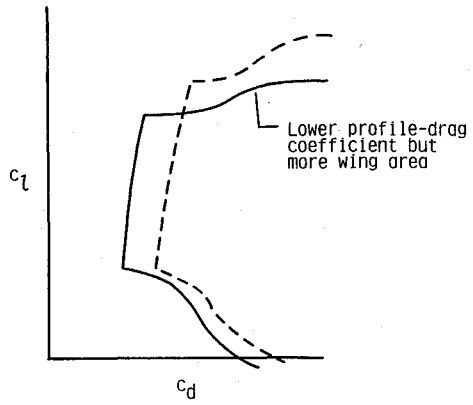

Fig. 3 Application of the figure of merit for directing the airfoil design process.

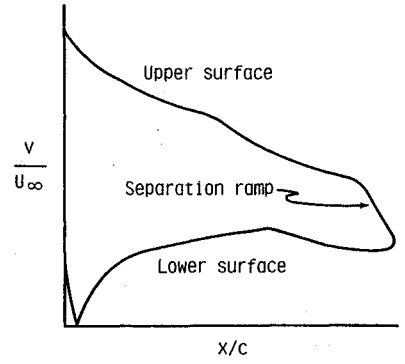

Fig. 4 Velocity distribution showing the separation ramp concept.

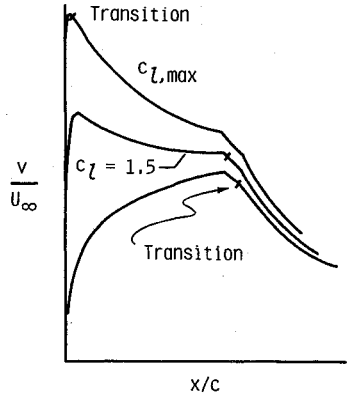

Fig. 5 Upper-surface velocity distribution behavior that achieves $c_{\ell,\max}$ independent of surface contamination.

The actual design of the airfoil was carried out using the Eppler program.[6,7] One of the most significant features of this method is its multipoint design capability. Using most other design methodologies, the airfoil is developed at a single operating point, then off-design conditions are explored, and, if unacceptable, the design-point solution is modified until acceptable off-design performance is achieved. The Eppler method, however, is unique in that the airfoil is designed to satisfy the performance envelope requirements from the outset. This is possible because it allows different parts of the airfoil to be designed for different operating conditions. In the case of the present airfoil, the upper surface is prescribed primarily for the upper limit of the low-drag range for $R = 0.7 \times 10^6$, which corresponds to the maximum endurance requirement, whereas the lower surface is prescribed for the

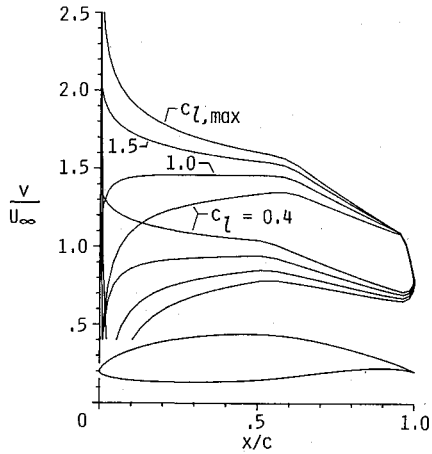

Fig. 6 NASA NLF(1)-1015 airfoil and inviscid velocity distributions.

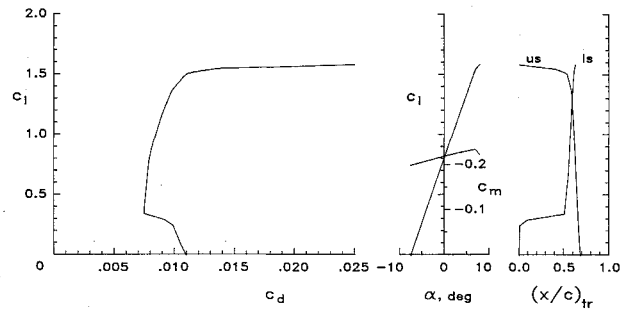

Fig. 7 Theoretical section characteristics of the NASA NLF(1)-1015 airfoil for the maximum endurance condition ($R = 0.7 \times 10^6$).

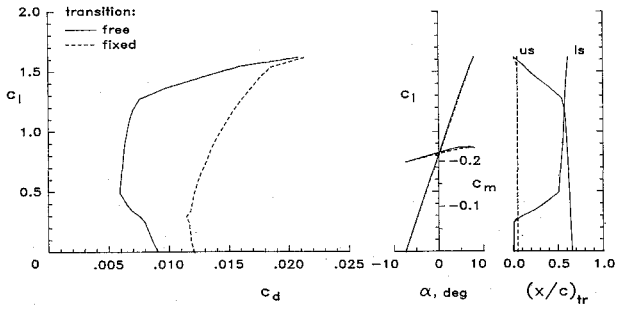

Fig. 8 Theoretical section characteristics of the NASA NLF(1)-1015 airfoil for the takeoff condition with transition free and transition fixed near the leading edge ($R = 2 \times 10^6$).

lower limit for $R = 2.0 \times 10^6$, which corresponds to the high-speed dash requirement.

It is also notable that unlike most other airfoil design methods, which determine the geometry that will generate a prescribed velocity distribution, the Eppler program provides the capability to go one step beyond this by allowing the shape of the airfoil to be dictated by the desired boundary-layer development.[8] Similarly, while the program lacks the capability of exactly modeling a laminar separation bubble which can strongly impact the aerodynamic characteristics, it does provide the designer with enough information to avoid such occurrences. Thus, not only was the present airfoil designed to avoid laminar separation bubbles that might be detrimental to performance, but also any bubbles that might introduce uncertainty into the prediction of the performance within the operating range were eliminated.

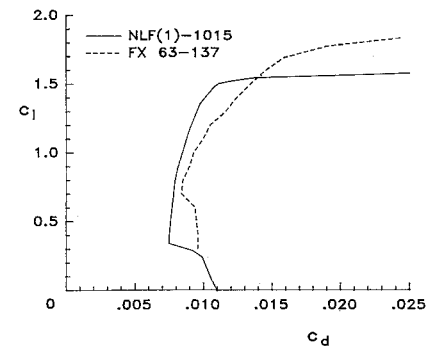

Fig. 9 Theoretical drag polar comparison of the NASA NLF(1)-1015 and Wortmann FX 63-137 airfoils ($R = 0.7 \times 10^6$).

Theoretical Results

The airfoil resulting from this design effort, along with the inviscid velocity distributions corresponding to key design lift coefficients, is presented in Fig. 6. This airfoil is designated as NASA NLF(1)-1015. The predicted section characteristics for the high-altitude, long-endurance operating condition are summarized in Fig. 7. In addition to the drag polar and the lift and pitching moment coefficients as they depend on angle of attack, this figure includes predictions of the transition locations as they vary with lift coefficient. A comparison of the drag polar prediction and the requirements shown in Fig. 2 indicates that all the performance goals have been satisfied.

The section characteristics with transition free and transition fixed near the leading edge for the Reynolds number corresponding to takeoff and landing are shown in Fig. 8. Most significant is the fact that the transition-free and transition-fixed polars merge at high lift coefficients. Thus, because the transition point on the upper surface has already moved to the leading edge, the behavior of the airfoil at high lift coefficients is independent of surface contamination. Based on long-term calibration of the Eppler program predictions against wind-tunnel and flight data, this airfoil is expected to have a maximum lift coefficient of about 1.8 for the takeoff and landing condition.

Comparison with Wortmann FX 63-137 Airfoil

Until now, the most promising airfoil for the high-altitude, long-endurance mission, has been the Wortmann FX 63 137.[9] In addition to having good performance at the appropriate Reynolds numbers, it benefits from having a maximum lift coefficient not affected by surface contamination. In order to provide a consistent comparison, the theoretical drag polar of this airfoil for $R = 0.7 \times 10^6$, which is in reasonable agreement with experimental results, is presented along with the polar of the NLF(1)-1015 airfoil in Fig. 9. The NLF(1)-1015 airfoil has lower drag everywhere within the range of interest. Although the Wortmann section is able to generate higher lift coefficients, these are of little use for the aircraft proposed, which, at altitude, does not operate at lift coefficients higher than the $c_\ell = 1.5$ specified for maximum endurance.

As the Reynolds number is increased from 0.7×10^6, the $c_{\ell,\max}$ of the Wortmann airfoil increases only slightly, whereas the increase for the NLF(1)-1015 airfoil is much greater. As the takeoff Reynolds number of 2.0×10^6 is reached, the $c_{\ell,\max}$ of the Wortmann airfoil is only about 0.1 greater than that predicted for the NLF(1)-1015 airfoil. As a consequence, the figure of merit is greater for the NLF(1)-1015 airfoil. With transition fixed near the leading edge, the characteristics of the two airfoils are predicted to be very similar.

Although the overall performance of the Wortmann airfoil is generally very good, that of the NLF(1)-1015 airfoil promises significant improvement along with greater thickness and less negative pitching moment.

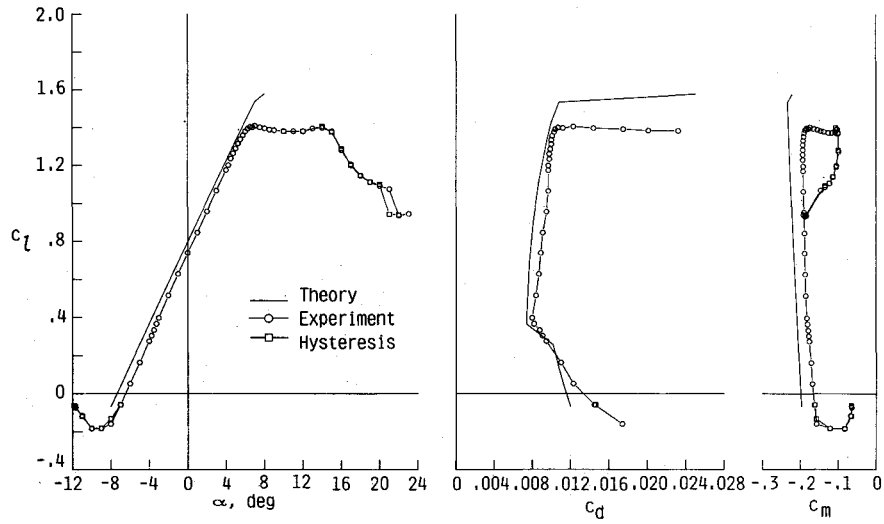

Fig. 10 Comparison of theoretical and experimental results for the maximum endurance condition ($R = 0.7 \times 10^6$).

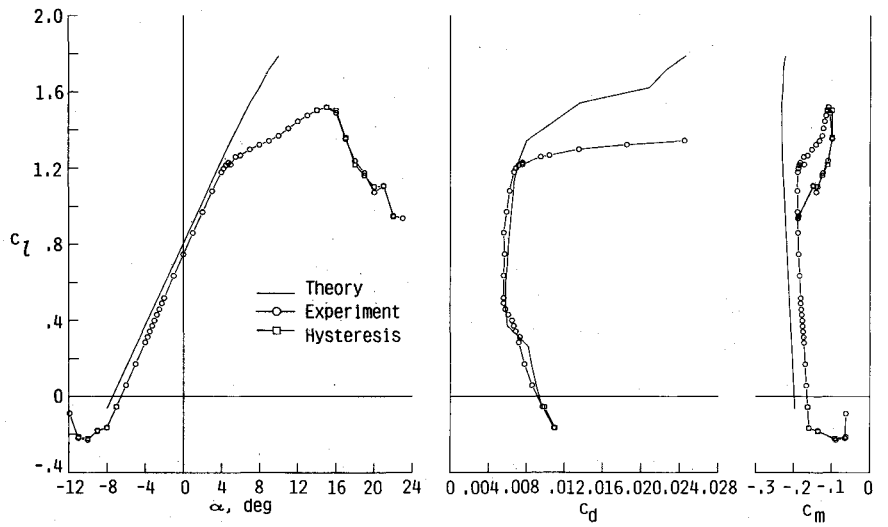

Fig. 11 Comparison of theoretical and experimental results for the takeoff condition ($R = 2 \times 10^6$).

Comparison of Theoretical and Experimental Results

In order to validate the design methodology of the NLF(1)-1015 airfoil, an investigation was conducted in the Low-Turbulence Pressure Tunnel at the NASA Langley Research Center. While no attempt is made here to report fully on these experiments, it is of interest to compare the experimental results with the theoretical predictions for the most important design points.

A comparison of the theoretical and experimental results for the maximum endurance condition ($R = 0.7 \times 10^6$) is presented in Fig. 10. The excellent stall behavior, characterized by an approximately constant c_ℓ over a nearly 10 deg angle-of-attack range, is notable. This behavior is attributable to the separation ramp concept. In general, the predicted and experimental results are in good agreement, although the theoretical $c_{\ell,\max}$ of 1.6 at this Reynolds number was not realized in the experiment. Also, while it was anticipated in the design process that the low-drag range would be narrower than predicted by $\Delta c_\ell = 0.07$ at each limit, the experimental results show that, in addition to this, the entire polar is shifted downward by a similar amount.

In considering the capability of the design method to account for laminar separation bubbles, it should be noted that the theoretical and experimental results should be expected to agree only at the upper limit of the low-drag range, as is the case. Based on experience with the program, significant laminar separation bubbles are expected at lower lift coefficients, causing the drag to be underpredicted at these points. This is of no consequence to the suitability of the airfoil, however, because only the lift coefficient at the upper limit of the low-drag range is in the operational flight envelope of the specified aircraft at this Reynolds number. At lower lift coefficients, the corresponding flight Reynolds numbers are higher and increased bubble drag is not predicted.

The theoretical and experimental results for the takeoff condition ($R = 2 \times 10^6$) are compared in Fig. 11. The predicted drag coefficients within the low-drag range are in excellent agreement with the measured values. As is the case for the lower Reynolds number, the value of $c_{\ell,\max}$ appears to be overpredicted. Unfortunately, the data available are insufficient to allow a conclusive explanation to be made for the discrepancy between the theoretical and experimental $c_{\ell,\max}$ values.

Conclusions

With present airfoil design capabilities, every new aircraft should have an airfoil tailored specifically to its mission requirements. Because the airfoil characteristics impact the aircraft design, however, the best match of the airfoil to the aircraft requires that the airfoil design be integrated with the design of the aircraft. The number of cycles in the resulting airfoil/aircraft iteration process are minimized by starting

with an airfoil that closely matches the design specifications. Thus, to provide realistic airfoil performance data to aid in the preliminary design and sizing of high-altitude, long-endurance aircraft, an airfoil suitable for such missions has been designed. This airfoil demonstrates that a substantial improvement in vehicle performance is possible through the use of a mission-specific airfoil designed taking advantage of the multipoint capability of the Eppler program.

Finally, the range of applicability of the Eppler airfoil design methodology has been extended. In particular, the ability to design airfoils for moderately low Reynolds numbers without significant laminar separation bubbles has been demonstrated.

References

[1]Mueller, T. J., "Low Reynolds Number Vehicles," AGARDograph 288, 1985.

[2]Liebeck, R. H., "Low Reynolds Number Airfoil Design at the Douglas Aircraft Company," *Proceedings of Conference on Aerodynamics at Low Reynolds Numbers,* Royal Aeronautical Society, London, Vol. 1, Paper 7, Oct. 1986.

[3]Evangelista, R., Pfenninger, W., Mangalam, S. M., and Bar-Sever, A., "Design and Wind Tunnel Test of a High Performance Low Reynolds Number Airfoil," AIAA Paper 87-2349, Aug. 1987.

[4]Maughmer, M. D. and Somers, D. M., "Figure of Merit for Airfoil/Aircraft Design Integration," AIAA Paper 88-4416, Sept. 1988.

[5]Somers, D. M., "Design and Experimental Results for a Flapped Natural-Laminar-Flow Airfoil for General Aviation Applications," NASA TP-1865, 1981.

[6]Eppler, R. and Somers, D. M., "A Computer Program for the Design and Analysis of Low-Speed Airfoils," NASA TM-80210, 1980.

[7]Eppler, R. and Somers, D. M., "Supplement To: A Computer Program for the Design and Analysis of Low-Speed Airfoils," NASA TM-81862, 1980.

[8]Maughmer, M. D. and Somers, D. M., "The Design of an Airfoil for a High-Altitude, Long-Endurance Remotely Piloted Vehicle," *NASA Symposium on Natural Laminar Flow and Laminar Flow Control Research,* NASA CP-2487, 1987, Vol. 3, pp. 777–794.

[9]Althaus, D. and Wortmann, F. X., *Stuttgarter Profilkatalog I,* Vieweg und Sohn, Braunschweig/Wiesbaden, FRG, 1981.